

High spin states in ^{68}As : Experiment and theory

A. Petrovici,^{1,2,3,4} K. W. Schmid,³ Amand Faessler,^{2,3} D. Pantelica,¹ F. Negoita,¹ B. R. S. Babu,⁴ A. V. Ramayya,⁴ J. H. Hamilton,⁴ J. Kormicki,^{4,5} L. Chaturvedi,^{2,4,6} W. C. Ma,^{4,*} S. J. Zhu,^{4,†} N. R. Johnson,⁷ I. Y. Lee,^{7,‡} C. Baktash,⁷ F. K. McGowan,⁷ M. L. Halbert,⁷ M. Riley,^{7,§} and J. D. Cole⁸

¹*Institute for Physics and Nuclear Engineering, R-76900 Bucharest, Romania*

²*Joint Institute for Heavy Ion Research, Oak Ridge, Tennessee 37831*

³*Institute für Theoretische Physik, Universität Tübingen D-72076 Tübingen, Germany*

⁴*Physics Department, Vanderbilt University, Nashville, Tennessee 37235*

⁵*UNISOR, ORISE, Oak Ridge, Tennessee 37831*

⁶*Department of Physics, Banaras Hindu University, Varanasi, India*

⁷*Oak Ridge National Laboratory, Oak Ridge, Tennessee 37831*

⁸*Idaho Nuclear Engineering Laboratory, Idaho Falls, Idaho 43415*

(Received 21 November 1995)

High spin states in ^{68}As have been studied using the $^{56}\text{Fe}(^{14}\text{N},2n)^{68}\text{As}$, $^{58}\text{Ni}(^{12}\text{C},pn)^{68}\text{As}$, and $^{46}\text{Ti}(^{25}\text{Mg},p2n)^{68}\text{As}$ reactions. New high spin states have been observed including a band structure above the known 2160 keV isomeric state. A microscopic description based on the EXCITED VAMPIR model for negative and positive parity states in ^{68}As is presented. A possible mechanism to populate the observed high spin isomeric state is proposed. The complex structure of the ^{68}As nucleus is caused essentially by specific shape coexistence effects. [S0556-2813(96)03405-2]

PACS number(s): 21.10.Re, 21.60.Jz, 25.70.Gh, 27.50.+e

I. INTRODUCTION

The extensive experimental and theoretical work on the structure of nuclei near $A=60-80$ has revealed many interesting features: large prolate deformations ($\beta\approx 0.4$); shape variation as a function of particle number, excitation energy, and spin [1,2]. Both the rapid changes in structure and shape coexistence reflect the competition between the neutron and proton shell gaps which occur at large oblate and prolate deformations near nucleon numbers 36 and 38. The coexistence of oblate and prolate deformed states, sometimes very strongly mixed, have been experimentally identified [1,3] and theoretically described [4-11] for a couple of nuclei in $A\sim 70$ region. Investigations of the odd-odd nuclei in this region are especially important since they should be particularly sensitive to changes of the proton-neutron interaction and the interplay between single-particle and collective degrees of freedom. Recently we made our first attempt to describe fully microscopically the yrast states [10] in an odd-odd nucleus, ^{72}As .

As part of a systematic study undertaken to investigate the structure of odd-odd As nuclei, the level scheme of ^{68}As was reinvestigated since there are many discrepancies in the published work. Prior to this work information on the excited levels of this nucleus was rather scarce: in particular, little

was known about high spin states in ^{68}As . The ground state spin and parity of ^{68}As was determined to be 3^+ from the study of the β^+ decay [12] of ^{68}As to ^{68}Ge and from the decay studies of ^{68}Se to ^{68}As [13]. Further preliminary information on low lying levels of ^{68}As comes from the study of radioactive decay [14] of ^{68}Se . Pardo [15] reported additional levels obtained from the study of $^{54}\text{Fe}(^{16}\text{O},pn\gamma)$ and $^{58}\text{Ni}(^{12}\text{C},pn\gamma)$ reactions. From the delayed γ rays observed using the same reactions, Raghavan *et al.* [16] identified a new isomeric state at 2160 keV in ^{68}As and measured $T_{1/2}$ and the g factor of the isomer. A compilation of the experimental data on the excited states of ^{68}As was updated by Bhat [17]. Level schemes of ^{68}As with considerable differences at high spins have been proposed [18,19] in unpublished annual reports based on the $^{12}\text{C}(^{58}\text{Ni},pn)^{68}\text{As}$ and $^{56}\text{Fe}(^{14}\text{N},2n)^{68}\text{As}$ reactions. Here we report the results from the studies of the $^{56}\text{Fe}(^{14}\text{N},2n)^{68}\text{As}$, $^{58}\text{Ni}(^{12}\text{C},pn)^{68}\text{As}$ and $^{46}\text{Ti}(^{25}\text{Mg},p2n)^{68}\text{As}$ reactions which extend our knowledge concerning the high spin states of ^{68}As .

In order to understand the structure of an odd-odd nucleus and determine the relevant degrees of freedom dynamically by the effective many-body Hamiltonian of the considered system, we use here the EXCITED VAMPIR approach [20]. In this approximation general symmetry-projected Hartree-Fock-Bogoliubov (HFB) quasiparticle determinants are used as trial configurations and the underlying mean fields as well as the configuration mixing are determined by a series of variational calculations.

We include neutron-proton as well as parity mixing in the mean field and use essentially complex HFB transformations. Imposing time-reversal and axial symmetry on the quasiparticle transformations we account for time-odd unnatural parity nucleon-nucleon correlations as well as both $T=0$ and $T=1$ neutron-proton pairing in the mean fields [20].

*Present address: Department of Physics, Mississippi State University, Mississippi State, Mississippi 39762.

†Present address: Physics Department, Tsinghua University, Beijing, People's Republic of China.

‡Present address: Lawrence Berkeley Laboratory, Berkeley, California 94720.

§Present address: Department of Physics, Florida State University, Tallahassee, Florida 32306.

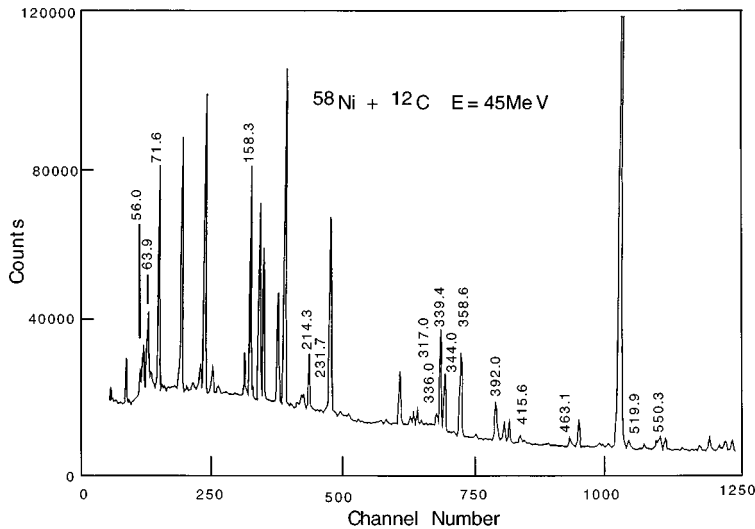


FIG. 1. The singles γ -ray spectrum in the energy range 0–600 keV obtained by using the reaction $^{58}\text{Ni}(^{12}\text{C},pn)^{68}\text{As}$ at 45 MeV beam energy.

An interesting problem posed to the theoretical models in this case is the presence [16] of an isomeric state at 2160 keV which is supposed to be a high spin state. The theoretical investigation presented here is an attempt to understand microscopically the structure of the positive and negative-parity states in ^{68}As and to find a possible description of the experimentally identified isomeric level.

II. EXPERIMENTAL PROCEDURES AND RESULTS

Excited states in ^{68}As were first investigated in three γ - γ coincidence experiments. In the first two experiments, states in ^{68}As were populated using the $^{56}\text{Fe}(^{14}\text{N},2n)^{68}\text{As}$ reaction at a beam energy of 46 MeV and the $^{58}\text{Ni}(^{12}\text{C},pn)^{68}\text{As}$ reaction at beam energies between 36 and 45 MeV. The calculations of fusion evaporation cross sections by means of the code CASCADE predict a rather strong population of ^{68}As in the $^{58}\text{Ni} + ^{12}\text{C}$ reaction (142 mb cross section for the pn channel at 40 MeV bombarding energy). The measurements were performed with ^{12}C and ^{14}N beams from the tandem Van de Graaff accelerator of the Institute for Physics and Nuclear Engineering in Bucharest. Two experiments were carried out with the purpose of determining excitation functions and γ - γ coincidences. The targets were metallic foils of natural Fe (91% ^{56}Fe) of 20 μm thick and ^{58}Ni (98%) of 15 μm thick. The γ rays were detected with two 120 cm^3 active volume Ge detectors. One of them was a HP Ge gamma-X, and the other was a Ge(Li) detector. The energy resolution was ~ 2.1 keV at 1.33 MeV.

In the third experiment we used the reaction $^{46}\text{Ti}(^{25}\text{Mg},p2n)^{68}\text{As}$ at a beam energy of 68 MeV. The population of high spin states was enhanced in this case because the maximum angular momentum brought into the compound system is considerably higher than that in the $^{58}\text{Ni}(^{12}\text{C},pn)^{68}\text{As}$ reaction. The target was a stack of three foils of total thickness 0.777 mg/cm^2 . The ^{25}Mg beam was provided by the tandem accelerator at the Holifield Heavy Ion Research Facility (HHIRF) in Oak Ridge. The γ -rays were detected with 19 Compton-suppressed Ge detectors in the spin spectrometer at HHIRF. The Ge detectors typically

had a resolution of 2.2 keV at 1.33 MeV and an efficiency of 25%.

III. SINGLES γ -RAY SPECTRA

Singles spectra were recorded with the GX detector placed at 55° to the beam direction. The spectrum measured in the $^{58}\text{Ni} + ^{12}\text{C}$ is complex since five residual nuclei $^{67}\text{Ga}(3p)$, $^{68}\text{Ge}(2p)$, $^{67}\text{Ge}(2pn)$, $^{68}\text{As}(pn)$, and $^{65}\text{Ga}(\alpha p)$ were produced with comparable yields in the decay of the compound nucleus ^{70}Se . The γ -ray spectrum in the energy of 0–600 keV is shown in Fig. 1. The energies of the transitions belonging to ^{68}As are marked in Fig. 1. Often one finds transitions of similar energies in neighboring nuclei giving rise to additional complications during data analysis. The relative yields of gamma rays were measured at ^{12}C beam energies of 36, 42, and 45 MeV. The 158.3 keV transition from the 158.3 keV level to the ground state was used for normalization. The yields are normalized to unity at 36 MeV. Figure 2 shows the γ -ray yields as a function of incident energy for some strong transitions. The increase in yield

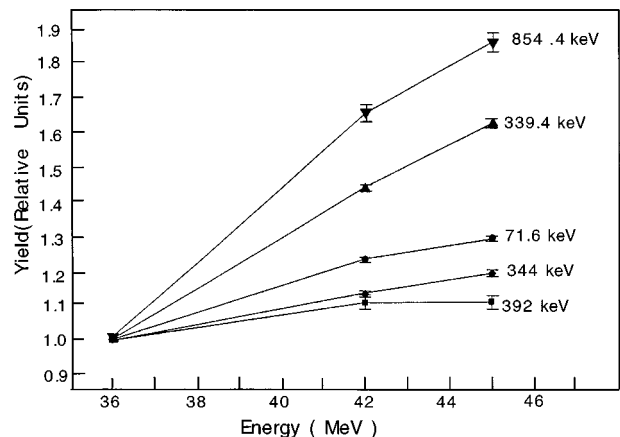


FIG. 2. The relative γ -ray yields as a function of incident energy using the reaction $^{58}\text{Ni}(^{12}\text{C},pn)^{68}\text{As}$. The yield for the 158.3 keV at 36 MeV is normalized to unity.

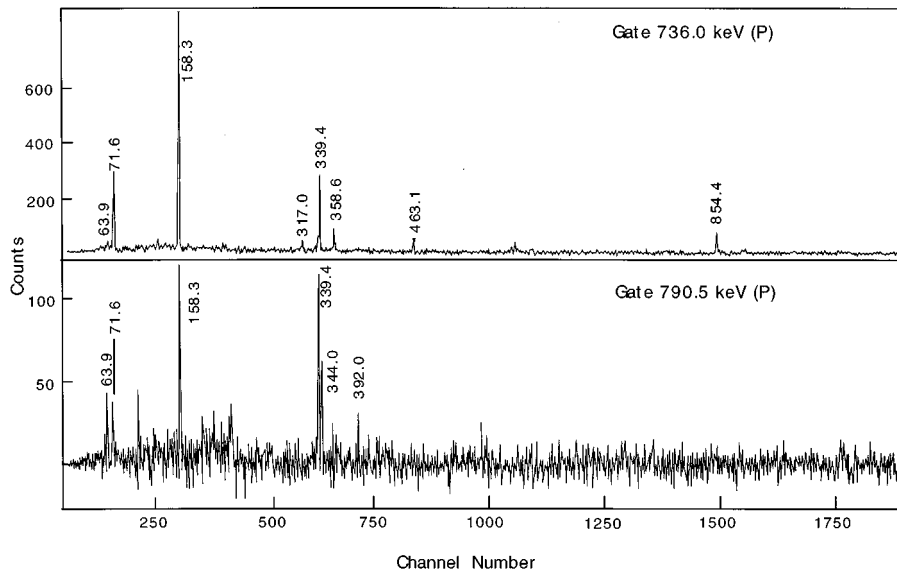


FIG. 3. The coincidence spectrum obtained by gating on the 736.0 and 790.5 keV transitions. *P* in parantheses denotes prompt coincidence spectrum.

and its shape as a function of bombarding energy suggests an ascending spin sequence. The measured transition intensities are indicated in Fig. 7 on the left side of the arrows.

IV. γ - γ COINCIDENCE MEASUREMENTS

The $^{58}\text{Ni} + ^{12}\text{C}$ coincidence experiment was performed at a beam energy of 45 MeV. The GX detector was placed at 90° and the Ge(Li) detector was placed at 120° to the beam axis. The coincidence data were sorted in a 4096×4096 two-dimensional array. Two digital gates were set on the time spectrum. The first window was set on the prompt time peak (the FWHM of the time spectrum was 20 ns), the second window corresponded to a delay of 80 ns. By using this procedure, the γ rays populating and deexciting isomeric states have been identified.

Figures 3–6 display γ - γ coincidence spectra with gates set on transitions in ^{68}As . The gamma rays are labeled with their energy in keV; *P* and *D* denote “prompt” and “delayed” coincidences, respectively.

In the $^{46}\text{Ti} + ^{25}\text{Mg}$ coincidence experiment the spin spec-

trometer multidetector array was used with a target detector distance of ≈ 21 cm. A total of 2×10^8 double- or higher-fold coincidence events were recorded. Many competing channels were present because of the high excitation energy and high angular momentum of the compound system. The γ - γ coincidence relationships and γ -ray intensities in the gates were used to construct the level scheme.

V. THE LEVEL SCHEME OF ^{68}As

On the basis of the γ - γ coincidence data the level scheme shown in Fig. 7 was constructed. The levels at 158.3, 214.3, 550.3, 734.2, 894.3, 965.9, 1305.3, and 1429.0 are already established and the results are summarized by Bhat [17]. Our coincidence data support the existence of these levels and the placements of the γ transitions between these levels. Our data do not support the existence of the levels at 313.2, 1119.8, 1195.1, 1215.2, and 1844 keV reported previously [17,18]. The γ transitions reported to depopulate these levels are not present in our γ spectra. In this section we present evidences for the new levels we propose in ^{68}As .

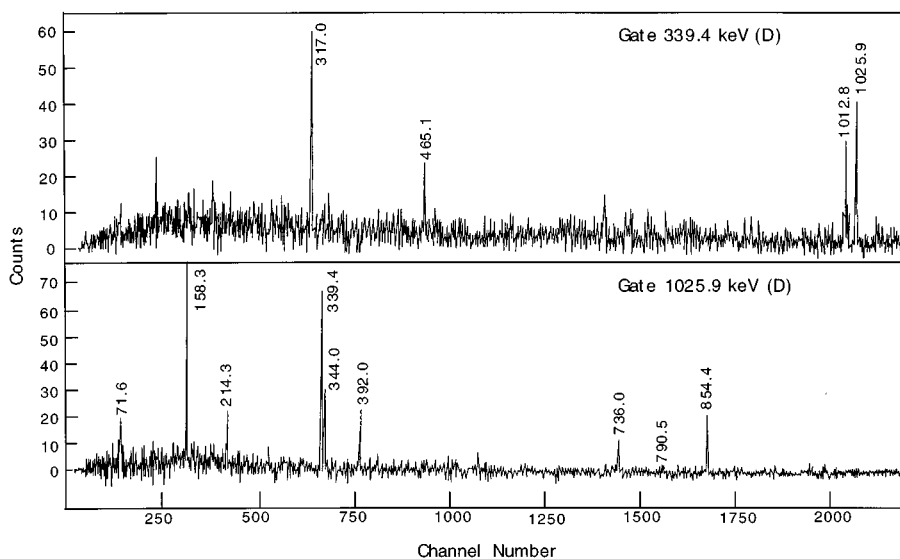


FIG. 4. The coincidence spectrum obtained by gating on the 339.4 and 1025.9 keV transitions. *D* in parantheses denotes delayed coincidence spectrum.

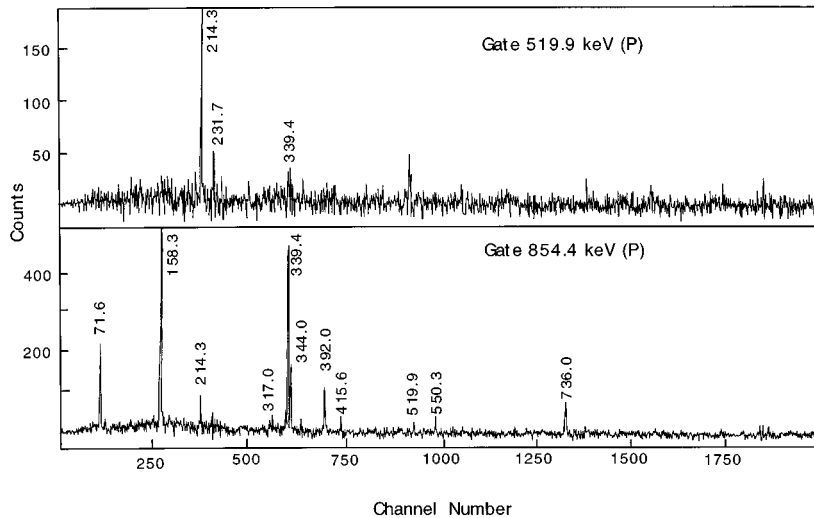


FIG. 5. The coincidence spectrum obtained by gating on the 519.9 and 854.4 keV transitions. *P* in parentheses denotes prompt coincidence spectrum.

Levels at 2095.8 and 2159.7 keV: In the coincidence spectrum gated with the 339.4 keV γ ray, the 63.9, 790.5, and 854.4 keV γ rays are seen. The 63.9 and 790.5 keV γ -rays are in coincidence with each other, but are not in coincidence with the 854.4 keV transition. Our γ - γ -coincidence data clearly show that the 790.5 keV γ ray is in coincidence with the 339.4 keV transition (see Fig. 3). These coincidence relationships establish these two levels. The placement is also supported by intensity and excitation function data. The isomeric character of the 2159.7 keV level [16] is also confirmed from our data.

From the analysis of our delayed γ - γ coincidence matrix the 317.0, 465.1, 1012.8, and 1025.9 keV γ rays are assigned to ^{68}As as deexciting levels above the isomeric level (see Fig. 4). From prompt and delayed coincidence relationships and γ -ray intensities in the gates for the 317.0, 465.1, 1012.8, and 1025.9 keV transitions, new levels at 2476.7, 2941.8, 3172.5, and 3185.6 keV are established. The first two levels are in one earlier annual report [18] and the first and last two in a later annual report [19]. Our results are supported by the $^{58}\text{Ni}+^{12}\text{C}$ and $^{46}\text{Ti}+^{25}\text{Mg}$ reaction data.

Levels at 1324.5 keV and 2303.5 keV: The level at 1324.5

keV is previously established [17]. Our coincidence data (obtained from $^{58}\text{Ni}+^{12}\text{C}$ and $^{46}\text{Ti}+^{25}\text{Mg}$ reactions) support the existence of this level. However, the 1326 keV transition tentatively placed on top of the 2303.5 keV level in an earlier report [18] is not observed in any of our reactions. Instead we observed a 979.0 keV transition to be in coincidence with 358.6 keV γ ray.

Levels at 2060.0 keV and 2935.0 keV: These two new levels are established from coincidence relationships and γ -ray intensities in the gates of the 463.1, 631.0, and 875 keV transitions using the $^{58}\text{Ni}+^{12}\text{C}$ and $^{46}\text{Ti}+^{25}\text{Mg}$ reactions. These levels appear in one annual report [18] but not in the other [19].

Level at 1956.9 keV: We introduced this new level following the observation of a 991.0 keV transition in coincidence with the 71.6 keV transition in the $^{46}\text{Ti}+^{25}\text{Mg}$ reaction data. In the coincidence spectrum gated with the 358.6 keV transition, a 632.4 keV transition is seen. The energy combination $632.4+358.6=991.0$ keV supports this placement. This level was reported in [18], but the 1026 keV transition placed on top of the 1956.9 keV level in [18] is misplaced. It is above the 2159.7 keV level.

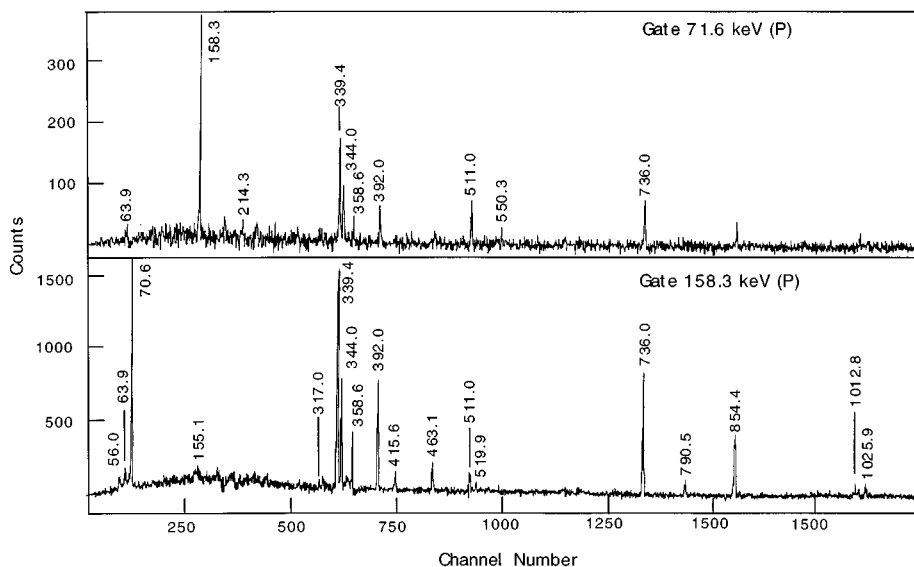


FIG. 6. The coincidence spectrum obtained by gating on the 71.6 and 158.3 keV transitions. *P* in parentheses denotes prompt coincidence spectrum.

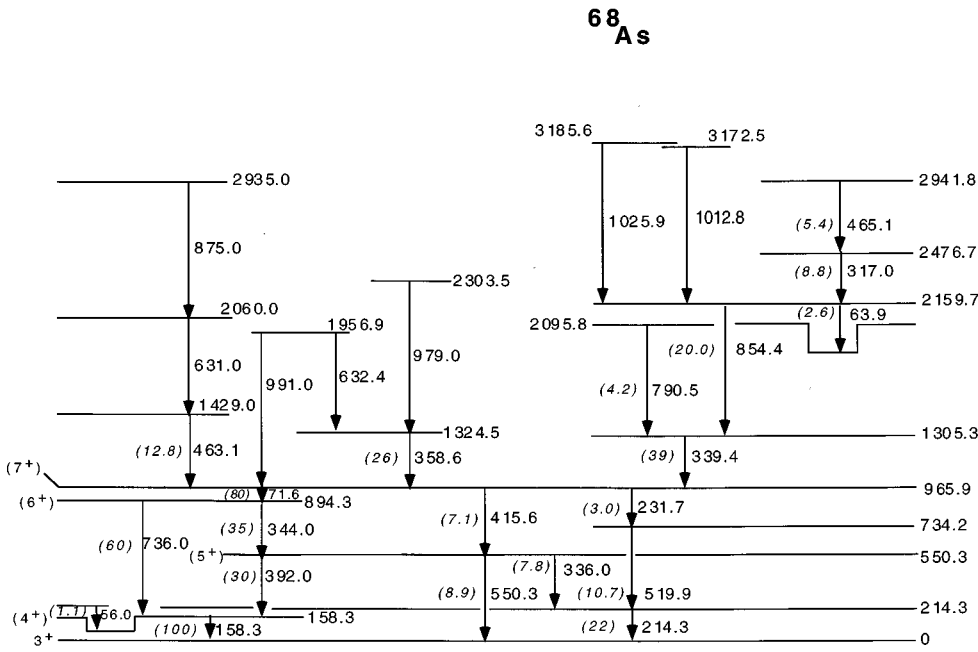


FIG. 7. Level scheme of ⁶⁸As.

We do not find evidence for the 4390 and 5089 keV levels above the 3172.5 and 3185.6 keV levels as reported earlier [19].

While definite spin and parity assignments require further measurements, some tentative spins can be assigned from the measured excitation functions.

The ground state spin and parity of ⁶⁸As were established to be 3^+ [12,13]. A spin change of two units between the ground state and the first excited state at 158.3 keV would result in a quite long lifetime (≥ 100 ns) for this level in disagreement with our results. So a spin and parity of $J=4^+$ is proposed for this level.

For the strongly populated levels at 550.3 keV and 894.3 keV, spin and parity assignments of 5^+ and 6^+ are proposed, respectively. The strong crossover transitions of 550.3 and 736.0 keV to ground and first excited states, respectively, clearly support a spin change of only one between the levels.

The excitation function and prompt coincidence relationships measured for the 71.6 keV transition gives a spin value of 7 for the level at 965.9 keV. By using the measured excitation functions for the 339.4 keV and 854.4 keV transitions, the spins of the 1305.3 keV and 2159.7 keV levels is expected to be > 7 .

The structures of odd-odd As nuclei are complex even at low spin. A change in structure is clearly observed when going from ⁷²As and ⁷⁰As to ⁶⁸As. An interesting new feature in ⁶⁸As is the high spin isomer. Additional measurements are necessary for definite spin and parity assignments and to establish the structure of the isomeric level.

VI. THEORETICAL RESULTS AND DISCUSSIONS

The results presented in this paper have been obtained using the most adequate effective Hamiltonian determined up to now for the $A \sim 70$ mass region adjusted by various variational calculations based on *complex* mean fields

[10,11]. With this Hamiltonian we have obtained a rather good description of the positive parity low spin states in ⁶⁸Ge nucleus [10], high spin negative parity bands in ⁶⁸Ge [9], the yrast positive and negative parity states in ⁷²As nucleus [10], and the shape transition and shape coexistence in several of $N \approx Z$ nuclei from krypton to molybdenum [11].

A ⁴⁰Ca core and a model space consisting of the $1p_{1/2}$, $1p_{3/2}$, $0f_{5/2}$, $0f_{7/2}$, $1d_{5/2}$, and $0g_{9/2}$ oscillator orbits for both protons and neutrons was used as single-particle basis states with the corresponding single-particle energies (in units of the oscillator energy $\hbar\omega$) 0.040, -0.270, 0.300, -0.560, 0.157, and 0.029 for the proton, and -0.070, -0.332, 0.130, -0.690, 0.079, and -0.043 for the neutron levels, respectively. For the bulk part of the effective two-body interaction we started with a nuclear matter G matrix derived from the Bonn one-boson-exchange potential [21] and made additional renormalizations: two short range (0.707 fm) Gaussians have been added to enhance the pairing correlations in the isospin $T=1$ proton-proton and neutron-neutron channels (the strengths are -40 MeV and -30 MeV, repectively). An additional Gaussian with the same range was introduced in the isoscalar spin 0 and 1 particle-particle channels (strength -180 MeV) to enlarge the neutron-proton G -matrix elements at low angular momenta, and an isospin-independent Gaussian-shape two-body spin-orbit force (range 0.5 fm, strength -1500 MeV) is also present. To influence the onset of deformation in the region some monopole shifts are introduced: a shift of -300 keV for all the diagonal isospin $T=0$ matrix elements of the form $\langle 0g_{9/2}0f; IT=0 | \hat{G} | 0g_{9/2}0f; IT=0 \rangle$ with $0f$ denoting either the $0f_{5/2}$ or the $0f_{7/2}$ orbit, and -500 keV in the $\langle 1p_{1d_{5/2}}; IT=0 | \hat{G} | 1p_{1d_{5/2}}; IT=0 \rangle$ matrix elements, where $1p$ denotes either the $1p_{1/2}$ or the $1p_{3/2}$ orbit.

We investigated positive and negative parity states in ⁶⁸As up to spin 16. First the vampir solutions, i.e., the mean field description of the yrast states with symmetry projection before variation [20], based on intrinsically prolate and ob-

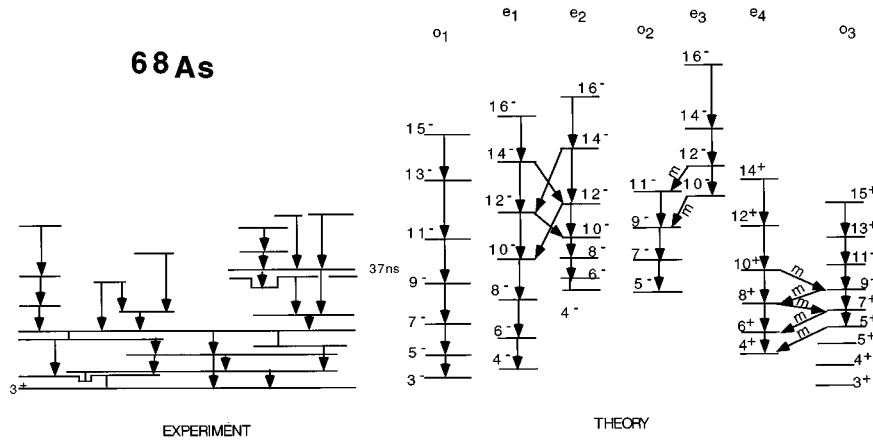


FIG. 8. The theoretical spectrum of the positive and negative parity states in the ^{68}As nucleus obtained within the *complex EXCITED VAMPIR* approach is compared with the available experimental data. The labels classifying the various theoretical bands are explained in the text. Indices m indicate significant $\Delta I=1$ $M1$ transitions. The even spin bands are labeled as e_1 , e_2 , e_3 , and e_4 and the odd spin bands as o_1 , o_2 , and o_3 .

late deformed trial configurations have been constructed. Different results have been obtained for the positive and negative parity yrast states. For the positive parity low spin states the oblate and prolate minima are almost degenerate or very close in energy and few additional local minima are found not too high in energy with respect to the deepest ones for both signs of the quadrupole deformation. At intermediate and high spins the situation is changed. The oblate minimum is here at least 1 MeV higher than the prolate one and its excitation energy increases further with increasing spin. For negative parity states the prolate minimum is at least 2.0 MeV deeper than the oblate one for all investigated spins. Thus the oblate-prolate shape coexistence is found only for the positive parity states in ^{68}As . However, these coexisting states are only weakly mixed via the Hamiltonian. The strong prolate-oblate mixing dominating the low spin states in some neighboring even-even nuclei is not found in the odd-odd nucleus ^{68}As .

In order to get an idea about the possible structure of a high spin isomer we built in the next step the first few positive and negative parity states for each considered spin in the frame of the *EXCITED VAMPIR* approach [20]. With this procedure every additional excited state of a given symmetry is constructed by an independent variational calculation imposing orthogonality with respect to the already obtained solutions and finally diagonalizing the residual interaction between them. In this way we build the optimal solutions for the lowest m states of a given spin parity (the yrast and the first $m-1$ excited states) in a m -dimensional space of A -nucleon configurations. It turned out that for the positive parity states, starting with spin 8, for each spin the first excited state is at least 1.2 MeV higher than the yrast one and then a bunch of 3–4 states are situated in an excitation energy interval smaller than 1 MeV. For the odd negative parity states, a similar picture was obtained. The even spin negative parity states manifest a different behavior starting with spin 12. The lowest three minima for 12^- , 14^- , and 16^- states are bunched in less than 650 keV excitation energy. On the other hand at low spins an energy gap of at least 1.2 MeV is found between the yrast and the first excited state for both even and odd spins. The physical states are obtained by diagonalizing the residual interaction between the lowest calculated symmetry-projected configurations. Investigating the electromagnetic decay pattern of the states calculated in this approximation we found that the different behavior of

the high spin negative parity states with respect to the low spin ones could cause the appearance of an isomeric state at intermediate spins.

In Fig. 8 we present the theoretical spectrum compared with the available experimental data. All the calculated states indicated in Fig. 8 are linear combinations of intrinsically prolate deformed states excepting for the lowest 3^+ , 5^+ , 6^+ and the first two 4^+ states. The 3^+ state and the lowest 5^+ state are based on intrinsically oblate deformed mean fields. The first (second) 4^+ state is mainly oblate (prolate) deformed with a small mixing (7%) coming from intrinsically prolate (oblate) deformed configurations. The lowest 6^+ state is 97% a symmetry-projected configuration which is prolate deformed in the *intrinsic* system and 3% mixing of oblate deformed configurations. Starting with spin 7 the positive parity yrast states presented in Fig. 8 are based on prolate deformed configurations of more than 91%.

For the calculated negative parity states the configuration mixing is negligible for all spins with $I^\pi \leq 8^-$. Less than 10% mixing was found for the lowest three 10^- states. Starting with spin 12^- a very strong mixing was found. The structure of the wave functions for the calculated states indicate 23–38% mixing for 12^- states, 17–38% for 14^- states and 17–48% for 16^- states.

However, the states can still be classified into bands according to the $B(E2)$ values of the transitions.

The strong variations in the mixing of the states is reflected by the irregular level spacing of the bands and also explain the appearance of a second decaying branch with a significant $B(E2)$ strength. The secondary branches indicated in Fig. 8 represent 18–27% of the total $B(E2)$ value.

Since the calculations are done in a finite model space we introduced some phenomenological renormalizations. For the quadrupole moments and electric transitions the effective charges of $1.5e$ for the protons and $0.5e$ for the neutrons and for the $M1$ operator the bare g factors of free nucleons have been used. For the $E1$ transitions connecting positive and negative parity states we are confronted with the problem of *spurious* admixtures due to the motion of the system as a whole. Because of numerical reasons, the projection into the center of momentum rest frame before variation cannot be performed. We eliminated the spuriousity from the $E1$ operator by introducing effective charges of $(N/A)e$ for the protons and $-(Z/A)e$ for the neutrons, respectively.

The theoretical values of the spectroscopic quadrupole moments obtained for the different states within the bands displayed in Fig. 8 give indication concerning not only the deformation of the states, but also on the strong mixing of configurations characterizing the structure of some states. For the positive parity even spin (band e_4) states, above 10^+ , the quadrupole moment ($Q_2^{\text{sp}} \sim -92 e \text{ fm}^2$) is larger than ($Q_2^{\text{sp}} \sim -85 e \text{ fm}^2$) for odd spins (band o_3). The $B(E2)$ values of ~ 94 W.u. for the levels above spin 10^+ have been obtained.

For the odd spin negative parity states (bands o_1 and o_2) the yrast states are more deformed ($Q_2^{\text{sp}} \sim -95 e \text{ fm}^2$) at higher spins, and a similar behavior is reflected by the in-band $B(E2)$ values. The $B(E2)$ values of ~ 100 W.u. for the corresponding yrast sequence, except for the $15^- \rightarrow 13^-$ transition which has a value of 86 W.u. For the second band (o_2) indicated in Fig. 8 $B(E2) \sim 78$ W.u. have been obtained.

The situation is different for the calculated even spin negative parity bands (labeled e_1 , e_2 , and e_3 in Fig. 8). The quadrupole moments indicate only small variations from one band to another. However, the second band (e_2) is the most deformed ($Q_2^{\text{sp}} \sim -92 e \text{ fm}^2$) above spin 12^- . The total $B(E2)$ strength is the highest above spin 12^- . For the e_1 , e_2 , and e_3 bands, the in-band $B(E2; 14^- \rightarrow 12^-)$ values are 56, 69, and 77 W.u., respectively. The crossing $E2$ branches indicated in Fig. 8 for the 14^- states are 3–4 times weaker than the main ones. The $B(E2)$ values for the $16^- \rightarrow 14^-$ transition in the e_1, e_2, e_3 bands are 80, 81, and 53 W.u. respectively. The $B(E2; 12^- \rightarrow 10^-)$ values are equal to ~ 68 W.u. for the first two bands. Changing the monopole shifts introduced in the effective two-body interaction to influence the onset of deformation in the region (from -300 keV to -375 keV for $T=0$ matrix elements discussed above) the conclusions concerning the deformation of the states and the influence of the mixing of configurations on the $E2$ decaying pattern is not changed.

Concerning the third even-spin negative parity band (e_3), starting already with spin 12^- , significant $M1, \Delta I=1$ transitions compete with the $E2$ branches. The $B(M1, \Delta I=1)$ values for the crossing transitions connecting the e_3 and o_2 bands are 70 m W.u., for the $12^- \rightarrow 11^-$ branch and 160 m W.u. for the $10^- \rightarrow 9^-$ branch. The yrast negative parity odd- and even-spin sequences are connected by $M1, \Delta I=1$ transitions characterized by almost constant $B(M1)$ strengths of the order of 20 m W.u. (these weaker transitions are not indicated in Fig. 8). For the positive parity states the $B(M1)$ values for even- to odd-spin transitions vary from 100 m W.u. to 300 m W.u., decreasing with increasing spin. They are almost a factor of 2 stronger for the transitions from odd to even spins.

Concerning the $E1$ transitions connecting the negative and the positive parity states we found $B(E1)$ values of the order of $10^{-4} - 10^{-5} e^2 \text{ fm}^2$ with small isoscalar components in the $7^+ \rightarrow 7^-$, $8^- \rightarrow 8^+$, $9^- \rightarrow 9^+$, $10^- \rightarrow 10^+$, $12^- \rightarrow 12^+$ transitions. The calculations indicate that the low spin positive parity states are connected with the negative parity ones by $E1$ transitions with $B(E1)$ values of the order of $10^{-4} - 10^{-5} e^2 \text{ fm}^2$. However they contain a large isos-

calar component and are probably strongly contaminated by spurious admixtures.

The shape mixing responsible for the particular behavior at high spins suggests a possible mechanism to produce an isomeric state at medium spins. According to the level spacings displayed in Fig. 8 the second 8^- state, being very close to the 6^- state becomes an isomeric level. The pattern of the bands displayed in Fig. 8 correlated with the calculated electromagnetic properties suggests that similar situations could be imagined for the second 9^- or 10^- . Present calculations give g factors of 0.62, 0.56, and 0.52 for the second 8^- , 10^- , and 9^- , respectively. The experimental g factor of 0.23(2) [16] for the isomeric level will require obviously considerable additional admixtures to lower the theoretical result to the available experimental value. Introducing additional determinants in the linear combinations for these states via the EXCITED VAMPIR procedure could change the relative positions of the intermediate spin states. Such an appreciable computational effort would require more detailed experimental information.

A second problem which we investigated is connected with the low spin behavior of the ^{68}As nucleus. Based on the above-described effective Hamiltonian within the limit of accuracy presently obtained using the excited vampir procedure we found that the yrast 3^+ state is below the 3^- state. A small change in the effective interaction could change the relative positions of the low spin positive parity states with respect to the negative parity ones.

Concerning the pairing correlations the calculations indicate that for all the states both isoscalar as well as isovector neutron-proton pairing have a significant contribution. This is also an indication that the neutron-proton interaction plays an important role for the structure of the odd-odd nuclei in the $A \sim 70$ mass region.

The complex behavior of the odd-odd nucleus ^{68}As is revealed by Excited vampir approach based on essentially complex HFB transformations. The shape coexistence is manifested for low- and high-spin, positive and negative parity states. Clear spin and parity assignments and also more information on the electromagnetic properties of the states are required before adventuring into more extensive calculations. Small changes in the effective interaction could cause considerable changes especially for weak electromagnetic transitions and for the picture displayed at low spins. New experimental investigations forseen in the near future will help the theoretical investigations to clarify at least part of the problems.

ACKNOWLEDGMENTS

Work at Vanderbilt University and Idaho National Engineering Laboratory were supported in part by the U.S. Department of Energy under Grant and Contract Nos. DE-FG05-88ER40407 and DE-AC07-76ID01570, respectively. Oak Ridge National Laboratory is managed by Martin Marietta Energy Systems, Inc. for the U.S. Department of Energy under Contract No. DE-AC05-84OR21400.

- [1] J. H. Hamilton, in *Treatise on Heavy-Ion Science*, edited by D. A. Bromley (Plenum, New York, 1989), Vol. 8, p. 3.
- [2] Proceedings on Nuclear Structure of the Zirconium Region, Bad Honnef, 1988, edited by J. Eberth, R. B. Mayer, and K. Sistemich (unpublished).
- [3] L. Chaturvedi *et al.*, Phys. Rev. C **43**, 2541 (1991).
- [4] A. Petrovici, K. W. Schmid, F. Grümmer, A. Faessler, and T. Horibata, Nucl. Phys. **A483**, 317 (1988).
- [5] A. Petrovici, K. W. Schmid, F. Grümmer, and A. Faessler, Nucl. Phys. **A504**, 277 (1989).
- [6] A. Petrovici, K. W. Schmid, F. Grümmer, and A. Faessler, Nucl. Phys. **A517**, 108 (1990).
- [7] A. Petrovici, K. W. Schmid, F. Grümmer, and A. Faessler, Z. Phys. A **339**, 71 (1991).
- [8] A. Petrovici, E. Hammarén, K. W. Schmid, F. Grümmer, and A. Faessler, Nucl. Phys. **A549**, 352 (1992).
- [9] A. Petrovici, K. W. Schmid, and A. Faessler, Z. Phys. A **347**, 15 (1993).
- [10] A. Petrovici, K. W. Schmid, and A. Faessler, Nucl. Phys. A **571**, 77 (1994).
- [11] A. Petrovici, K. W. Schmid, and A. Faessler, submitted to Nucl. Phys. A.
- [12] R. C. Pardo *et al.*, Phys. Rev. C **15**, 18811 (1977).
- [13] P. Baumann, M. Bounajma, A. Huck, G. Klotz, A. Knipper, G. Walter, G. Marguier, C. Richard-Serey, H. Ravn, E. Hagebø, P. Hoff, and K. Steffenson, Phys. Rev. C **50**, 1180 (1994).
- [14] P. Baumann *et al.*, Rapport d'activite, Strassbourg, 1989, p. 80.
- [15] R. C. Pardo, Ph.D. thesis, University of Texas at Austin, 1976.
- [16] P. Raghavan *et al.*, Bull. Am. Phys. Soc. **31**, 1210 (1986).
- [17] M. R. Bhat, Nucl. Data Sheets **55**, 1 (1988).
- [18] J. H. McNeill, A. A. Chishti, W. Gelletly, B. J. Varley, H. G. Price, C. J. Lister, O. Skeppstedt, and R. Broda, Manchester Nuclear Physics report 1987/1988, p. 17.
- [19] P. G. Bizzeti, A. M. Bizzeti-Sona, P. R. Maurenzig, D. Bazzacco, S. Lunardi, G. de Angelis, and A. Cardona, National Institute of Nuclear Physics, Legnaro National Laboratory Annual Report L.M.L.-I.N.F.N. (REP) 58/92, 1991, p. 9.
- [20] K. W. Schmid, F. Grümmer, and A. Faessler, Ann. Phys. **180**, 1 (1987).
- [21] K. Holinde, K. Erkelenz, and R. Alzetta, Nucl. Phys. **A194**, 161 (1972).